



# New wrinkling substrate assay reveals traction force fields of leader and follower cells undergoing collective migration



Sho Yokoyama <sup>a,1</sup>, Tsubasa S. Matsui <sup>a,b</sup>, Shinji Deguchi <sup>a,b,\*</sup>

<sup>a</sup> Department of Nanopharmaceutical Sciences, Nagoya Institute of Technology, Japan

<sup>b</sup> Division of Bioengineering, Osaka University, Japan

## ARTICLE INFO

### Article history:

Received 14 November 2016

Accepted 25 November 2016

Available online 27 November 2016

### Keywords:

Collective cell migration

Epithelial cells

MDCK-II cells

Traction force microscopy

Wrinkling substrate assay

## ABSTRACT

Physical forces play crucial roles in coordinating collective migration of epithelial cells, but details of such force-related phenomena remain unclear partly due to the lack of robust methodologies to probe the underlying force fields. Here we develop a method for fabricating silicone substrates that detect cellular traction forces with a high sensitivity. Specifically, a silicone elastomer is exposed to oxygen plasma under heating. Removal of the heat shrinks the substrate so as to reduce its critical buckling strain in a spatially uniform manner. Thus, even small cellular traction forces can be visualized as micro-wrinkles that are reversibly emerged on the substrate in a direction orthogonal to the applied forces. Using this technique, we show that so-called leader cells in MDCK-II cell clusters exert significant magnitudes of traction forces distinct from those of follower cells. We reveal that the direction of traction forces is highly correlated with the long axis of the local, individual cells within clusters. These results suggest that the force fields in collective migration of MDCK-II cells are predominantly determined locally at individual cell scale rather than globally at the whole cell cluster scale.

© 2016 Elsevier Inc. All rights reserved.

## 1. Introduction

Cells often move in cohesive groups during embryonic morphogenesis, wound repair, and cancer invasion. For better understanding of such collective cell behaviors, robust methodologies to probe underlying cellular traction force fields are helpful. To this end, fluorescent microbead-based traction force microscopy [1] and micropillar assay [2,3] have been developed to visualize cell-driven elastic deformations of the substrates. However, details regarding the whole view of multicellular traction force fields still remain elusive partly because these experiments and analyses are not always easy to practice.

Cellular traction forces were first visualized using wrinkling of deformable silicone substrates [4]. In this method, prepolymer silicone fluid was coated on a cell culture dish and polymerized by contacting with a burner flame for a few seconds so that micro-wrinkles were generated on the planar surface upon exertion of

traction forces. This technique is not suited to strictly quantifying the traction forces with a unit of Newton or Pascal because of complicated mechanical analyses of the wrinkle generation. Besides, the local burner treatment would result in yielding spatially nonuniform material properties. Consequently, the sensitivity to forces to display wrinkles would be heterogeneous in space, thus inappropriate for observing wide-spanned collective cell migration. Yet, the wrinkling technique has a huge merit of allowing for direct visualization of cellular forces as wrinkles in a manner promptly observed with conventional transmitted light microscopy.

Here we describe a method to modify the wrinkling substrate technique to improve the reproducibility and spatial homogeneity. We use oxygen plasma to create a thin oxide layer on a silicone elastomer in a reproducible and spatially uniform manner. The hydrophilic surface layer is mechanically stiffer compared to the underlying silicone solid and thus becomes buckled to display wrinkles when compressive stress is loaded. We also improve the sensitivity of the substrate to detect even small traction forces to expand the range of application to various cell types. Using this spatially uniform and highly force-sensitive substrate, we investigate traction force fields of epithelial cells undergoing collective migration.

\* Corresponding author. Division of Bioengineering, Graduate School of Engineering Science, Osaka University, 1-3 Machikaneyama, Toyonaka, Osaka 560-8531, Japan.

E-mail address: [deguchi@me.es.osaka-u.ac.jp](mailto:deguchi@me.es.osaka-u.ac.jp) (S. Deguchi).

<sup>1</sup> Present address: Micro/Nano Technology Center, Tokai University, Japan.

## 2. Results and discussion

### 2.1. Highly sensitive substrate enables detection of contractile forces of various cell types

We previously reported a method to detect cellular contractile forces as wrinkles with a pitch of subcellular length-scale, which was initially applied to MTD-1A epithelial cells elsewhere [5] and here characterized in details to demonstrate its usefulness in studying various cell types.

Cell culture dishes supporting a silicone solid were treated with oxygen plasma under heating (Fig. 1A, i–iii). We directly measured with light microscopy that the substrate thermally expands with this heating (Fig. 1B). The thermal expansion strain increased up to  $\sim 6 \times 10^{-4}$  at 50 °C, corresponding to an expansion of 6  $\mu\text{m}$  if the reference length is 10 mm. The removal of the heating back to the room temperature (24 °C; Fig. 1A, iv) results in generation of wrinkles on the substrate surface because of the following reasons: with the oxygen plasma treatment, the surface stiffened compared to the original state, implying that the range of elastic deformation is accordingly narrowed to some extent. Because the removal of the initial heating is followed by the shrink to the original length, a compression is loaded onto the substrate to induce buckling. Cell experiments are usually performed at 37 °C, and this moderate thermal expansion from the room temperature to the experimental condition again flattens the surface (Fig. 1A, v). Plating cells at this condition promptly elicits wrinkles on the surface because of the cellular intrinsic contraction (Fig. 1A, vi).

Our methodology is summarized as follows: assuming the reference length to be  $L$  (i), the substrate is modified with plasma under heating where the length is now  $L + \delta_1$  due to thermal expansion (ii, iii). Returning the length to  $L$  at the room temperature is followed by generation of wrinkles (iv), but those wrinkles again disappear at the warmer temperature where cells are cultured because a slight thermal expansion of  $\delta_2$  is added (v). In this last condition, wrinkles are generated sensitively and locally where traction forces are applied by cells (vi). Here we determined the heating temperature 60 °C (and resulting expansion  $\delta_1$ ) to planarize the substrate surface just at the culture temperature 37 °C. This process minimizes the buckling strain, which is a threshold compressive strain required for causing wrinkling. Consequently, the sensitivity to cellular forces is significantly improved as shown

below.

To evaluate the sensitivity, three distinct types of proliferative cells are used, i.e. mesenchymal (MEF, mouse embryonic fibroblasts), epithelial (MDCK-II, Madin–Darby canine kidney), and sarcoma (U2OS, human osteosarcoma) cells. Cells were seeded on the substrate at room temperature and placed in a stage incubator at 37 °C (Fig. 1C). Initially just after starting the imaging, isotropic wrinkles were observed all over the substrate because the dish is still close to room temperature, i.e., at condition iv in Fig. 1A. Here, the isotropic wrinkles are generated because the plasma is illuminated uniformly onto the substrate, and then a planar compression after the removal of heating is loaded on the round dish in a center-symmetric manner. As the temperature increased up to 37 °C, the random wrinkles gradually disappeared where cells were absent. Meanwhile, at the other places in the proximity of cells, wrinkles are rearranged to become oriented toward the cell axis as they were originated from pulling of the substrate by the individual cells. This traction force-induced wrinkling occurs on the substrate in an elastic, i.e. repeatable manner.

We quantified the sensitivity of the substrate to contractile forces, or specifically the percentage of how many cells generate wrinkles (Fig. 2). Most MEF ( $\sim 90\%$ ) generated wrinkles even without the heating process. Meanwhile, only limited amounts ( $\sim 10\text{--}20\%$ ) of MDCK-II and U2OS cells generated wrinkles on the substrates manufactured with oxygen plasma but without the heating process. Yet, marked wrinkles were observed even for these cells ( $\sim 70\text{--}80\%$ ) if the dishes were manufactured with the thermal expansion process. These results indicate that, to detect cellular forces from the wrinkling, the heating process is dispensable for the mesenchymal cell types that exhibit marked traction forces on the substrate, but practically effective for the epithelial and cancer cells that exhibit relatively weaker forces.

### 2.2. Distinct force magnitudes between leader and follower cells

Traction force fields in collective migration of MDCK-II cells were previously investigated with the fluorescent microbead-based traction force microscopy [1], but this report did not focus on the mechanical role of so-called leader cells that take on mesenchymal cell-like morphology and large size [6–9]. Applying the present technique to observations of MDCK-II cell colonies, we found that leader cells that appear at the edge of their populations exert significant levels of traction forces distinct from those of follower cells (Fig. 3A). Because the substrate is spatially uniform in mechanical and chemical properties (Fig. 1), the present microscopy allows for visualization of the relative magnitude of traction forces among the cells imaged. Here, leader cells take on mesenchymal cell-like features not only for the apparent morphology but also for the presence of significant magnitudes of physical forces.

Intense wrinkles with clear stripe patterns are created under and at the front of leader cells (Fig. 3A). Morphology of leader cells always elongates in parallel along the border of cell clusters. The wrinkles just below the leader cells are orthogonal to the long axis of the cells, whereas those at the front run outward radially. Thus, the wrinkles just under cells are produced by centripetal “pinching” due to cellular contraction, whereas those at the outside of cells are caused by the pulling of the substrate toward the contracting cells and consequent Poisson’s effect. Under follower cells, weaker but still obviously distinguishable wrinkles are observed over the range of the cells located within  $\sim 1\text{--}20$  cell rows behind the leader cells. The angle between the long axis of follower cells and the direction of principal wrinkles under the cells was also almost normal, which will be discussed below regarding their specific contributions to the traction force fields (Fig. 4).

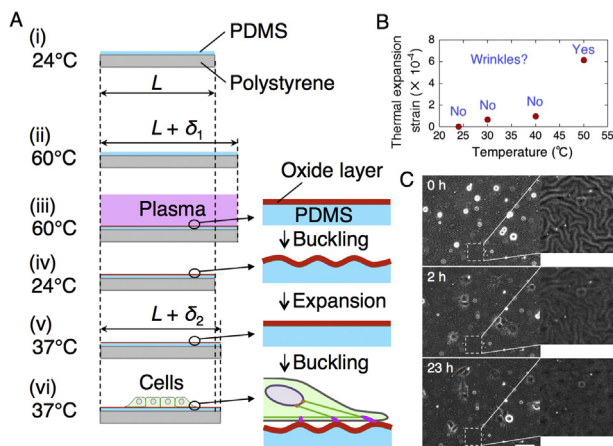


**Fig. 1. Force-sensitive substrate.** (A) Process for manufacturing the substrate. See text for details. (B) Wrinkles are generated on the substrate even in the absence of cells with a heating pretreatment up to more than 50 °C because a high thermal expansion strain is induced at Step iii in A. (C) Live imaging of U2OS cells on the substrate. Scale, 50  $\mu\text{m}$ .

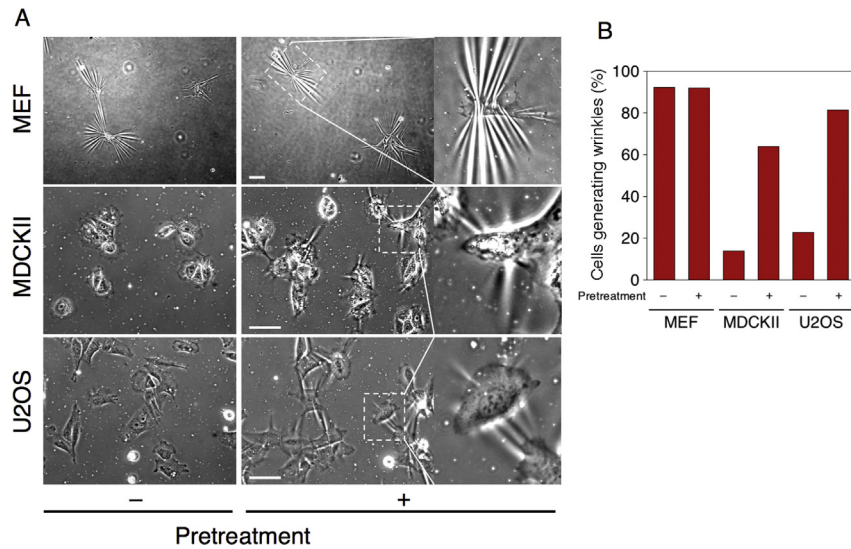


**Fig. 2.** Sensitivity of the substrate to cellular contractile forces. (A) The heating pretreatment is dispensable for MEF to generate wrinkles on the substrate, while highly improves the sensitivity for MDCK-II and U2OS cells. Scales, 50  $\mu\text{m}$ . (B) Percentage of cells generating clear wrinkles on the substrate, examined for each of the three cell types.

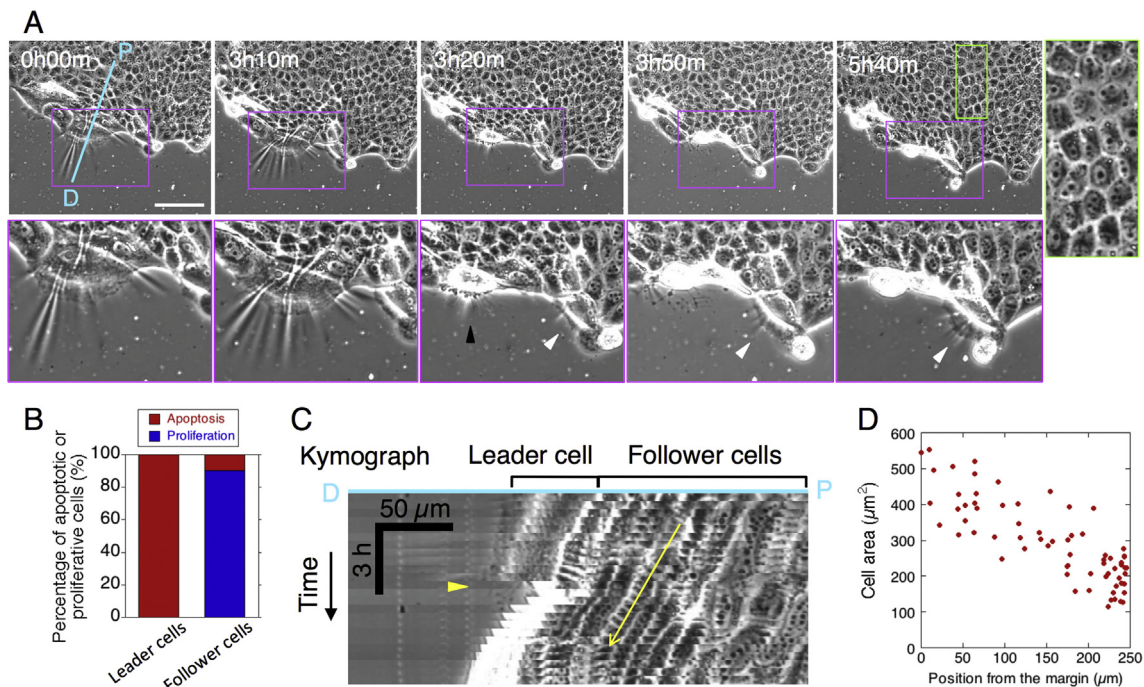


**Fig. 3.** Leader cells tend to undergo apoptosis with little effect on the collective migration speed. (A) Live imaging. Magenta-boxed areas are enlarged below to show apoptosis of a leader cell (black arrowhead) and a newborn leader cell (white arrowhead). Green-boxed area is magnified on the right to show representative appearance of submarginal cells. Scale, 100  $\mu\text{m}$ . (B) Percentage of apoptotic or proliferative cells in the leader or follower cells that became round in shape to detach from the substrate. Leader cells undergo apoptosis ( $n = 22$  cells,  $N = 3$  experiments). In contrast, the majority of follower cells undergo growth ( $n = 110$  cells), while the rest ( $n = 12$  cells) gets apoptosis (totally  $n = 122$  cells,  $N = 3$  experiments). (C) Kymograph along P–D (proximal–distal) line shown in A. The leader cell underwent apoptosis at a time indicated by the arrowhead, but the migration speed was not influenced as shown by the arrow with a constant slope ( $\sim 0.16$   $\mu\text{m}/\text{min}$ ). (D) Projected areas of cells inside of colonies are small compared to those around the margin. (For interpretation of the references to colour in this figure legend, the reader is referred to the web version of this article.)

### 2.3. Leader cells frequently undergo apoptosis but affect only limitedly the whole cluster movement

We found that leader cells never divide for proliferation but instead die in an apoptotic manner, while follower cells often divide but rarely ( $\sim 10\%$ ) die during collective migration (Fig. 3B). There is a possibility that accumulation of cellular signals originated from the profound traction forces may trigger the apoptosis. This tendency

of leader cells to apoptosis was not as remarkable in previous studies using collagen gel substrates [8] possibly because in our study no particular extracellular matrix (ECM) was coated in advance, but cell adhesiveness is ensured by the oxygen plasma-based hydrophilization and ECM components contained within the culture media. In this regard, our system allows for separating the roles of biochemical (i.e., ECM) and mechanical (i.e., softness of the substrate) contributions.

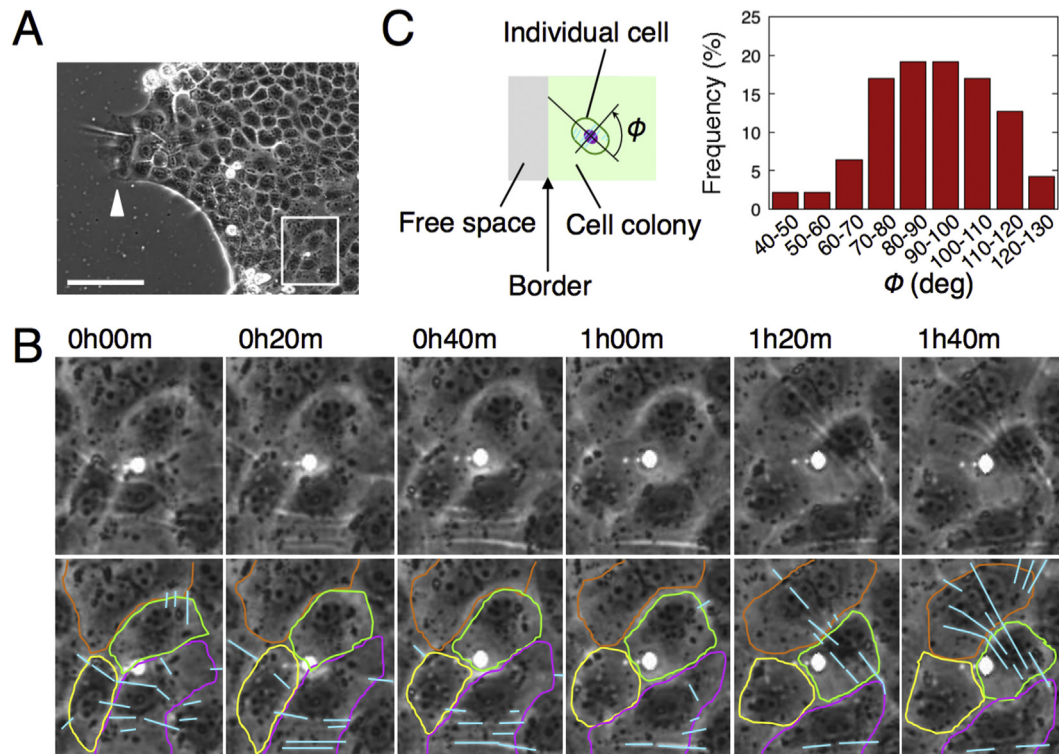


**Fig. 4. Traction force fields within cell colonies are determined by local cells.** (A) Collectively migrating cells analyzed. The arrowhead represents a leader cell. Scale, 100  $\mu\text{m}$ . (B) Time course of cells boxed in A. Some cells are outlined in the lower panels that are identical to the upper panels, with wrinkles marked in cyan. (C)  $\phi$  represents the angle between the cellular long axis and principal wrinkle direction. The right panel shows the frequency of  $\phi$  ( $0^\circ \leq \phi \leq 180^\circ$ ; investigated for  $n = 47$  cells,  $N = 3$  experiments; mean,  $92^\circ$ ). (For interpretation of the references to colour in this figure legend, the reader is referred to the web version of this article.)

After the death of leader cells, new cells that locate in the proximity enlarge and start to exert marked traction forces, thus transforming into a new leader cell, and then collective cell migration persists. We quantified the speed of the collective migration during these events (Fig. 3C), showing that no significant change occurs even with the apoptosis-based turnover of leader cells. This result suggests a limited role of leader cells in collective migration that they do not necessarily propel the cell cluster behind them. Our observation is sharply in contrast to the conclusion drawn previously based on the micropillar assay [3]. The apoptosis might be induced to exclude leader cells (acquiring apparently mesenchymal cell features) for self-protection of the epithelial system. In other words, because the mesenchymal cell-like leader cells may be produced via a partial EMT (epithelial-mesenchymal transition) that precedes tumor progression [9], the apoptosis may work as a form of epithelial defense against cancer [10,11].

Our observations are also in contrast to the previous study [8] that collective migration was temporarily suppressed when leader cells were manually removed using a pipette. This discrepancy may result from that our observations are accompanied by spontaneous apoptosis other than artificial removal of leader cells. Although leader cells may function to locally guide the direction of migration [8], our results show that even if leader cells spontaneously leave the group, the whole cluster moves persistently, and soon new leader cells are born at the cluster edge for some reason.

#### 2.4. The traction force fields within the cell cluster are determined by local individual cells

Our observations on MDCK-II cells were partly inconsistent with a previous study on the same cell lines [1] reported as follows: traction forces were high near the margin of cell colonies, and they

gradually decreased toward the inside of the cluster, but a small level of traction  $\sim 5$  Pa was maintained; consequently, this previous study concluded that the cell colonies engage in a global tug-of-war, and tractions transmitted all the way from cell-to-cell are accumulated up to more than 1 kPa within the cell cluster.

We found that the angle between the long axis of follower cells and local wrinkles is almost orthogonal (Fig. 4). Given that those wrinkles under cells are produced by contraction-driven centripetal pinching, this result supports that the force fields are determined by the local force balance ranging the scale of individual cells rather than the global force balance ranging the scale of cell colonies. If the global force balance at colony length scale is instead predominant, wrinkles would run in parallel along the cell colony border, which is the case for MTD-1A epithelial cells as this cell line has highly strong cell–cell contacts [5,12].

On the one hand, it was rare to see wrinkles deep inside cell colonies, thus having some regional preference. To explain the cause of this global scale difference, we focused on the cell size, which gradually reduced from the edge to the inside of cell colonies (Fig. 3D). Marginal (low-density) cells have apparently brighter cell–cell contacts in phase-contrast images compared to central (high-density) cells. The bright cell–cell contacts would reflect a valley-shaped cell topography and relatively immature cell–cell contacts. Meanwhile, the darker, smooth appearance conversely reflects a relatively flat topography and mature, firm cell–cell contacts. As marginal cells are close to the free space outside of the colony, they may be prone to take on spread morphology. Given that contractile forces in MDCK cell clusters are reported to be conserved between the cell–cell and cell–substrate adhesions [13], the marginal cells with less mature cell–cell contacts may by nature generate greater traction forces at the cell–substrate adhesions compared to central cells. Consequently, marginal and central

cells may take on different phenotypes, with the former generating a greater magnitude of wrinkles. Thus, we propose for MDCK-II cells that larger traction forces present near the edge of cell colonies are produced due to the inherent properties of marginal cells with spreader morphology. Meanwhile, central cells located deep inside the colonies are by nature different from the marginal cells in phenotype, exerting less detectable traction forces on the substrate. Indeed, the spontaneous detachment of apoptotic leader cells has almost no effect on the wrinkles under follower cells. Besides, a recent study [5] has demonstrated that particular molecules play a crucial role in coordinating collective cell migration by changing cell characters between marginal and submarginal cells. In contrast, the previous study [1] submitting the importance of global force balance did not consider the difference in biological phenotypic properties between the spread marginal and small central cells.

### 3. Materials and methods

#### 3.1. Cell culture

MEF (a gift from N. Kioka, Kyoto Univ.), MDCK-II cells (ECACC), and U2OS cells (ATCC) were seeded on a dish supporting the wrinkle substrate described below and cultured in high-glucose (4.5 g/L) DMEM (Gibco) supplemented with 10% FBS (SAFC Biosciences) and 1% penicillin-streptomycin (Wako). The dish was placed for passage in a 5% CO<sub>2</sub> incubator at 37 °C or for experiments in a stage incubator (5% CO<sub>2</sub>, 37 °C; Tokai Hit) mounted on an inverted microscope (IX71, Olympus; ORCA-R2, Hamamatsu).

#### 3.2. Force-sensitive substrate

The surface of a 35-mm-diameter polystyrene dish (Iwaki) was coated at room temperature (24 °C) using a spin-coater with a silicone elastomer (Sylgard 184, Dow Corning Toray) supplied as two-part liquid kits composed of polymer-base and curing agents and in advance oven-cured after mixing at a weight ratio of 100: 1. For surface modification, the dish was heated in an oven at 60 °C to induce thermal expansion of the whole dish and then exposed to oxygen plasma (4 mA, 600 V, 20 Pa, 1 min) using a glow discharge-typed plasma generator (SEDE-GE, Meiwafofos). An oxide layer was created on the substrate surface with a thickness of ~60 nm [14] and an elastic modulus of ~7.1 kPa as separately measured with a stainless steel ball-induced deformation analyzed by the Hertz model.

#### 3.3. Sensitivity of the substrate

To quantify thermal expansion of the substrate, we put the dish supporting the substrate in an oven for sufficient duration to the equilibrium, and the dish was quickly imaged outside the oven by phase-contrast microscopy (CKX41, Olympus; Moticam 1000, Motic). Local changes in the distance between neighboring small stains, which are inevitably present in the silicone elastomer [15] but can be used as a fiducial marker, were analyzed using ImageJ (NIH). Here thermal expansion is quantified as  $(d_1 - d_0)/d_0$  where  $d_0$  and  $d_1$  represent the distances between two fiducial markers at 24 °C and at the oven temperature, respectively.

To evaluate the sensitivity of the substrate to detect cellular contractile forces, either MEF, MDCK-II cells, or U2OS cells were sparsely cultured on the substrate. The percentage of cells generating wrinkles was quantified. MDCK-II and U2OS cells have a relatively short cell cycle so that they tend to exist as a cluster rather than individually. For these cells, we counted cell clusters

that are composed of less than 5 cells as a single group, and analyzed the percentage for each group. For MEF, we analyzed the percentage for individual cells.

#### 3.4. Analysis of collective cell migration

Phase-contrast images of MDCK-II cells were taken for more than 12 h at an interval of 10 min. Image analysis was performed to count the percentage of apoptotic or proliferative cells in the cells that shrank to detach from the substrate permanently or temporarily, respectively. Kymograph for evaluating the collective migration speed was constructed along an inspected line drawn perpendicular to a cell colony edge. We analyzed correlation in the angle between the cellular long axis and local wrinkles. The cellular long axis was obtained with ImageJ (NIH) by manually tracing cell outlines and using the ellipse fitting, and the direction of wrinkles was also quantified by manually tracing them with the same software.

### Acknowledgments

The authors thank Genki Ikeda and Taiki Ohishi for their assistance in determining the elastic modulus of the substrate. This study was partly supported by KAKENHI grants from the MEXT of Japan (#26750140, 15H03004, 15H06627, 16H05907, and 16K12872).

### Transparency document

Transparency document related to this article can be found online at <http://dx.doi.org/10.1016/j.bbrc.2016.11.142>.

### References

- [1] X. Trepat, M.R. Wasserman, T.E. Angelini, et al., Physical forces during collective cell migration, *Nat. Phys.* 5 (2009) 426–430.
- [2] O. du Roure, A. Saez, A. Buguin, et al., Force mapping in epithelial cell migration, *Proc. Natl. Acad. Sci. U. S. A.* 102 (2005) 2390–2395.
- [3] M. Reffay, M.C. Parrini, O. Cochet-Escartin, et al., Interplay of RhoA and mechanical forces in collective cell migration driven by leader cells, *Nat. Cell Biol.* 16 (2014) 217–223.
- [4] A.K. Harris, P. Wild, D. Stopak, Silicone rubber substrata: a new wrinkle in the study of cell locomotion, *Science* 208 (1980) 177–179.
- [5] A. Sakane, S. Yoshizawa, M. Nishimura, et al., Conformational plasticity of JRAB/MICAL-L2 provides “law and order” in collective cell migration, *Mol. Biol. Cell.* 27 (2016) 3095–3108.
- [6] T. Omelchenko, J.M. Vasiliev, I.M. Gelfand, et al., Rho-dependent formation of epithelial “leader” cells during wound healing, *Proc. Natl. Acad. Sci. U. S. A.* 100 (2003) 10788–10793.
- [7] H. Haga, C. Irahara, R. Kobayashi, et al., Collective movement of epithelial cells on a collagen gel substrate, *Biophys. J.* 88 (2005) 2250–2256.
- [8] N. Yamaguchi, T. Mizutani, K. Kawabata, H. Haga, Leader cells regulate collective cell migration via Rac activation in the downstream signaling of integrin  $\beta 1$  and PI3K, *Sci. Rep.* 5 (2015) 7656.
- [9] P. Friedl, D. Gilmour, Collective cell migration in morphogenesis, regeneration and cancer, *Nat. Rev. Mol. Cell Biol.* 10 (2009) 445–457.
- [10] M. Kajita, K. Sugimura, A. Ohoka, et al., Filamin acts as a key regulator in epithelial defence against transformed cells, *Nat. Commun.* 5 (2014) 4428.
- [11] M. Kajita, Y. Fujita, EDAC: epithelial defence against cancer–cell competition between normal and transformed epithelial cells in mammals, *J. Biochem.* 158 (2015) 15–23.
- [12] A. Sakane, A.A. Abdallah, K. Nakano, et al., Rab13 small G protein and junctional Rab13-binding protein (JRAB) orchestrate actin cytoskeletal organization during epithelial junctional development, *J. Biol. Chem.* 287 (2012) 42455–42468.
- [13] V. Maruthamuthu, B. Sabass, U.S. Schwarz, M.L. Gardel, Cell-ECM traction force modulates endogenous tension at cell-cell contacts, *Proc. Natl. Acad. Sci. U. S. A.* 108 (2011) 4708–4713.
- [14] T. Ohishi, H. Noda, T.S. Matsui, et al., Tensile strength of oxygen plasma-created surface layer of PDMS, *J. Micromech. Microeng.* 27 (2017) 015015.
- [15] S. Deguchi, J. Hotta, S. Yokoyama, T.S. Matsui, Viscoelastic and optical properties of four different PDMS polymers, *J. Micromech. Microeng.* 25 (2015) 097002.